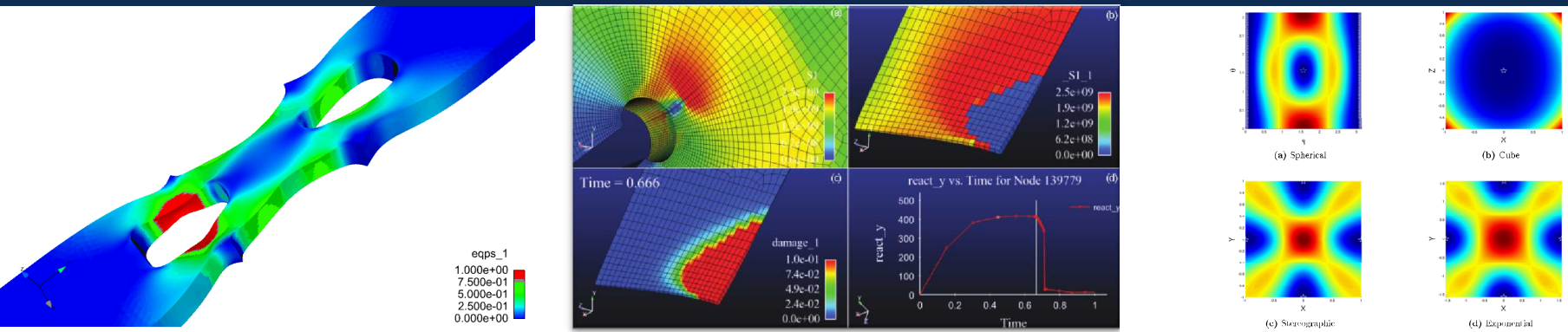


*Exceptional service in the national interest*



Jakob T. Ostien, James W. Foulk III, Alejandro Mota, Qiushi Chen, WaiChing Sun

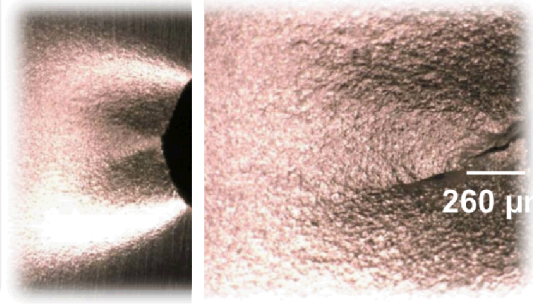
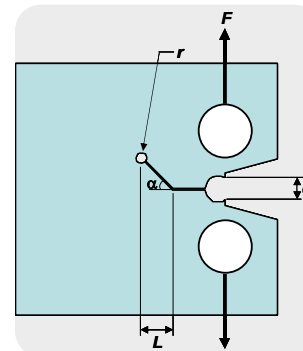
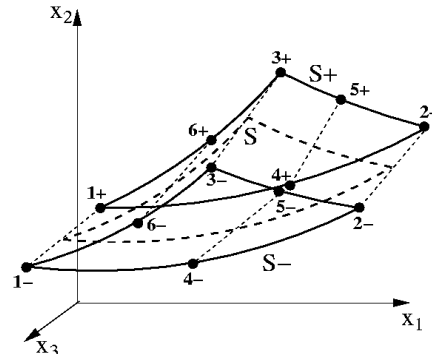
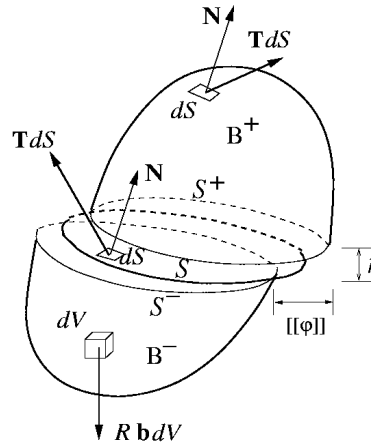


Sandia National Laboratories is a multi-program laboratory managed and operated by Sandia Corporation, a wholly owned subsidiary of Lockheed Martin Corporation, for the U.S. Department of Energy's National Nuclear Security Administration under contract DE-AC04-94AL85000. SAND NO. 2011-XXXX

# Outline

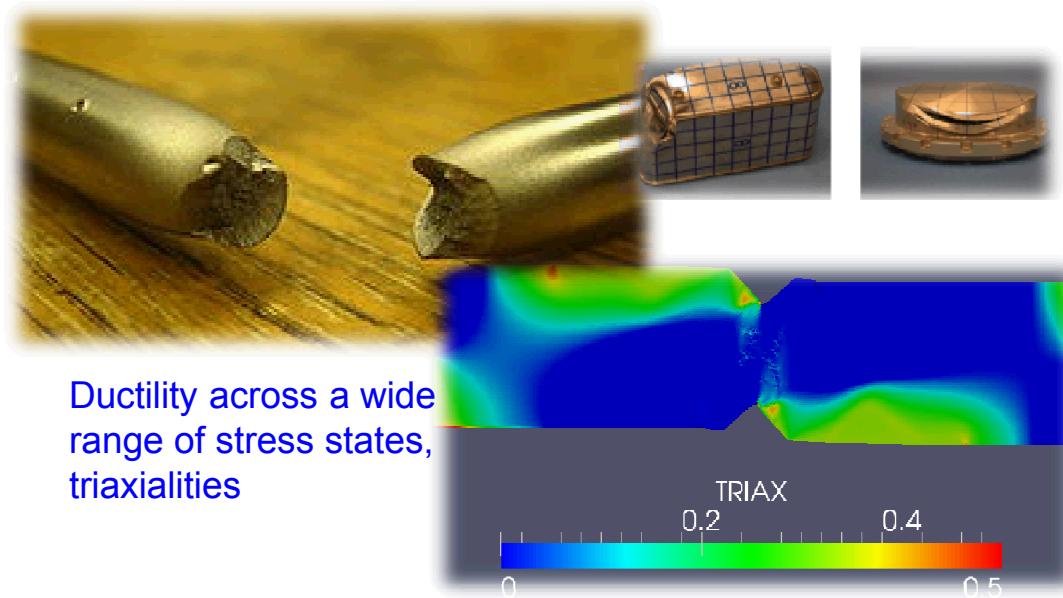
- Motivating problems in continuum multiscale plasticity
  - Modeling fracture and failure
  - Good finite elements are required to resolve stress states
  - Constitutive models must capture necking and plastic localization (global instabilities)
- Convergent numerical methods for models with local damage require *regularization* → *Nonlocal methods, surface elements*
  - Material (local) instabilities, loss of ellipticity, indicate localization and/or failure
- Continuum-to-Continuum Coupling
- Summary and Conclusions

# Modeling Fracture and Failure

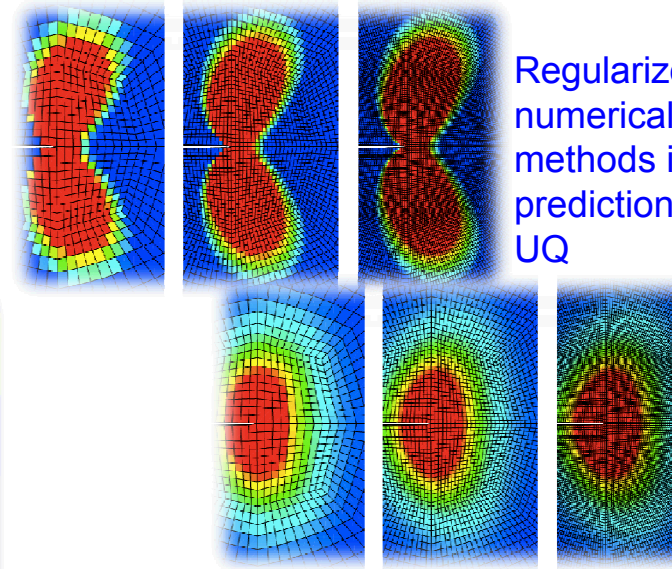


Ductile failure experiments, courtesy Brad Boyce via Sandia X-Prize

Finite element formulations for localization phenomena



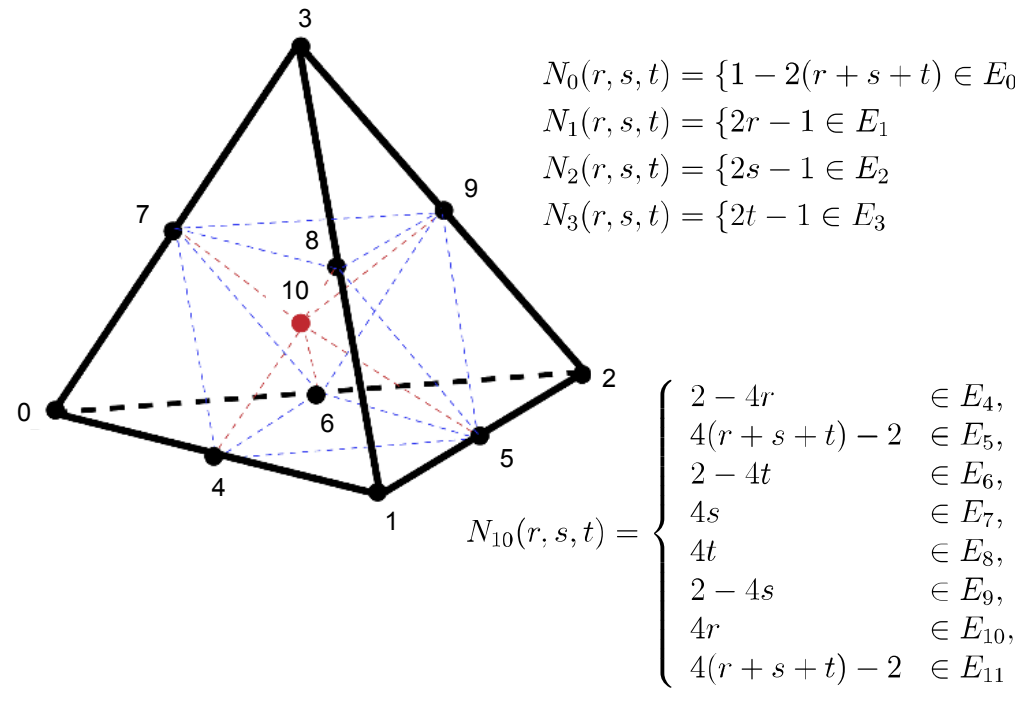
Ductility across a wide range of stress states, triaxialities



Regularized numerical methods improve predictions and UQ

# Finite Elements

- 10 noded tetrahedral element, Thoutireddy et al 2002.
- Multilinear basis with assumed linear spaces for deformation gradient and stress stemming from a three field Hu-Washizu variational principle



$$N_4(r, s, t) = \begin{cases} 2r & \in E_0, \\ 2 - 2(r + s + t) & \in E_1, \\ 1 - 2(s + t) & \in E_4 \cup E_7 \cup E_8 \cup E_{11} \end{cases}$$

$$N_5(r, s, t) = \begin{cases} 2s & \in E_1, \\ 2r & \in E_2, \\ 2(r + s) - 1 & \in E_4 \cup E_5 \cup E_8 \cup E_9 \end{cases}$$

$$N_6(r, s, t) = \begin{cases} 2s & \in E_0, \\ 2 - 2(r + s + t) & \in E_2, \\ 1 - 2(r + t) & \in E_8 \cup E_9 \cup E_{10} \cup E_{11} \end{cases}$$

$$N_7(r, s, t) = \begin{cases} 2t & \in E_0, \\ 2 - 2(r + s + t) & \in E_3, \\ 1 - 2(r + s) & \in E_6 \cup E_7 \cup E_{10} \cup E_{11} \end{cases}$$

$$N_8(r, s, t) = \begin{cases} 2t & \in E_1, \\ 2r & \in E_3, \\ 2(r + t) - 1 & \in E_4 \cup E_5 \cup E_6 \cup E_7 \end{cases}$$

$$N_9(r, s, t) = \begin{cases} 2t & \in E_2, \\ 2s & \in E_3, \\ 2(s + t) - 1 & \in E_5 \cup E_6 \cup E_9 \cup E_{10} \end{cases}$$

# Constitutive Models

- Introduce an internal state variable to govern statistically stored dislocations, homogenization of slip system response
- Pose a hardening minus recovery evolution equation for the isotropic hardening variable with a rate and temperature dependent flow rule

$$\dot{\epsilon}_p = f \left\{ \sinh \left[ \frac{\bar{\sigma}}{(1-\phi)(\kappa+Y)} - 1 \right] \right\}^n$$

Bammann, Chiesa, Johnson,  
Regueiro, Marin, Brown, et al

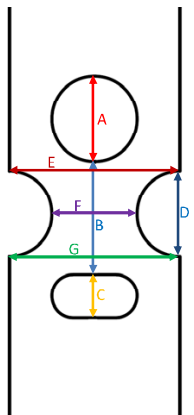
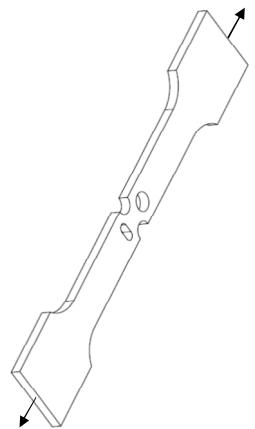
$$\dot{\kappa} = [H - R_d \kappa] \dot{\epsilon}_p$$

- Add state variables to capture the presence of voids in the matrix, with evolution equations for the size of the voids at a material point

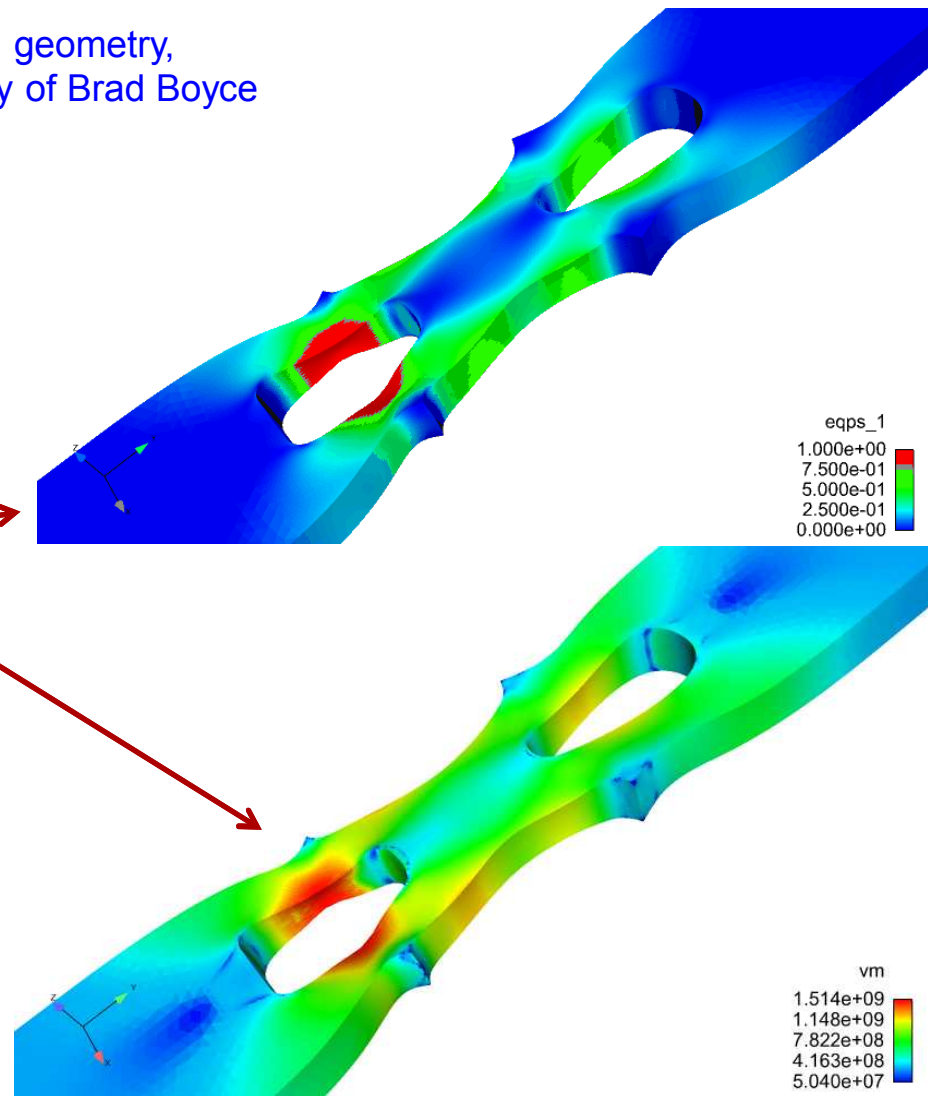
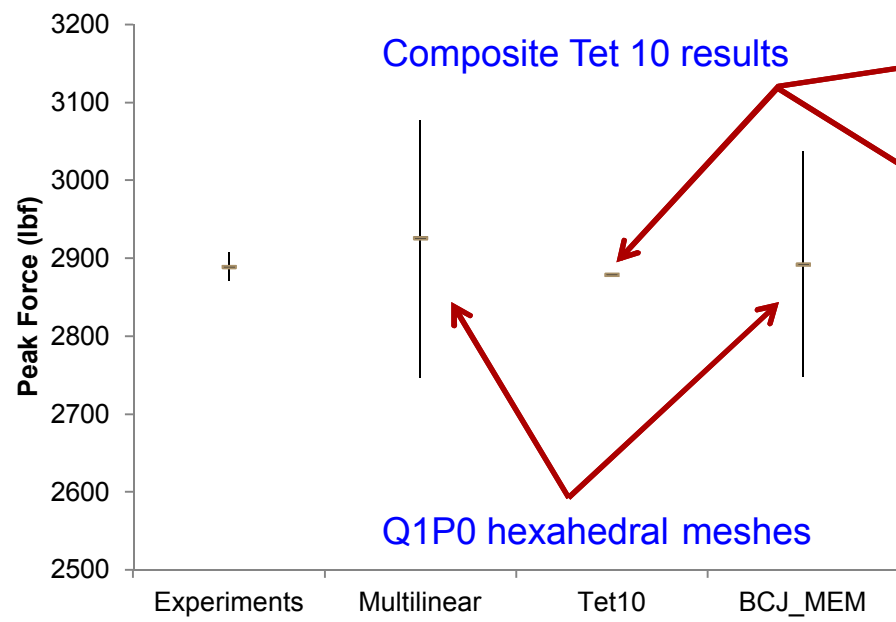
$$\dot{\phi} = \left\{ \frac{1}{(1-\phi)^m} - 1 \right\} \sinh \left[ \frac{2(2m-1)}{2m+1} \frac{\langle p \rangle}{\bar{\sigma}} \right]$$

Cocks and Ashby, 1980

# Representative Results



Sandia X-Prize geometry,  
results courtesy of Brad Boyce



# Regularization

## ■ Nonlocal methods

$$\Phi[\boldsymbol{\varphi}, \bar{\mathbf{Z}}, \bar{\mathbf{Y}}] := \int_B W(\mathbf{F}, \bar{\mathbf{Z}}, \mathbf{Q}, T) dV + \int_B \bar{\mathbf{Y}} \cdot (\bar{\mathbf{Z}} - \mathbf{Z}) dV - \int_B \rho_0 \mathbf{B} \cdot \boldsymbol{\varphi} dV - \int_{\partial_T B} \mathbf{T} \cdot \boldsymbol{\varphi} dS$$

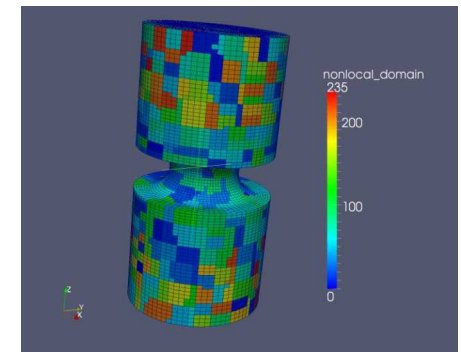
$$\begin{aligned} \int_B \mathbf{P} \cdot \text{Grad } N_a dV - \int_B \rho_0 \mathbf{B} N_a dV - \int_{\partial_T B} \mathbf{T} N_a dS &= \mathbf{0}, \\ \bar{\mathbf{Y}} &= \lambda_\alpha \left( \int_B \lambda_\alpha \lambda_\beta dV \right)^{-1} \int_B \lambda_\beta \mathbf{Y} dV, \\ \bar{\mathbf{Z}} &= \lambda_\alpha \left( \int_B \lambda_\alpha \lambda_\beta dV \right)^{-1} \int_B \lambda_\beta \mathbf{Z} dV, \end{aligned}$$

Euler-Lagrange equations

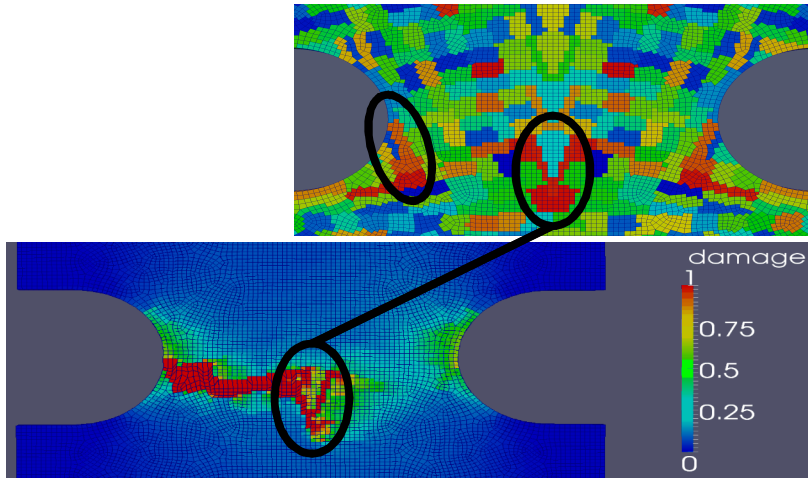


$$\begin{aligned} \bar{\mathbf{Y}} &= \frac{1}{\text{vol}(D)} \int_D \mathbf{Y} dV, \\ \bar{\mathbf{Z}} &= \frac{1}{\text{vol}(D)} \int_D \mathbf{Z} dV, \\ \text{vol}(\bullet) &:= \int_{(\bullet)} dV, \end{aligned}$$

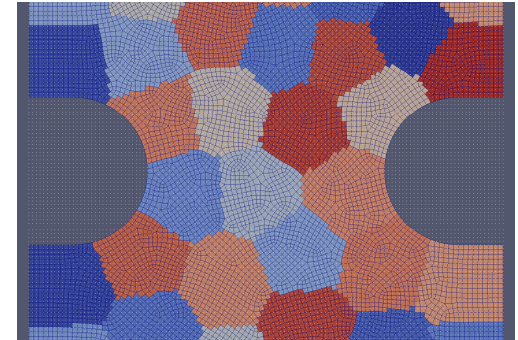
Nonlocal volumes created on processor



Length scale comes from the nonlocal volume



Domain decomposition algorithms can give poorly shaped volumes (left), a solution may be centroidal Voronoi tessellation (right)



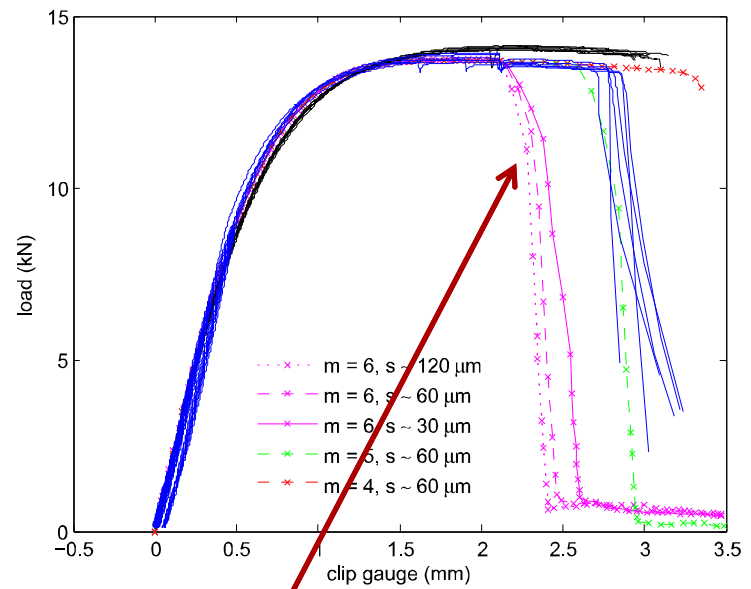
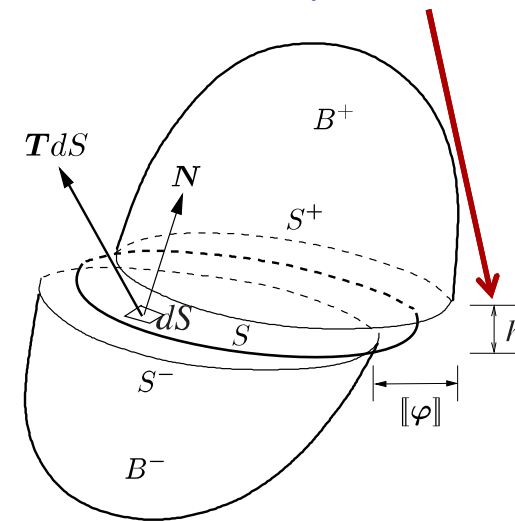
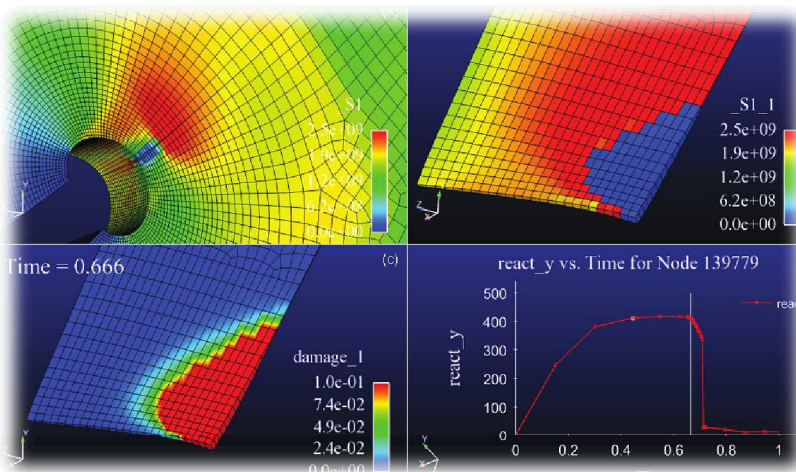
Foulk, Mota, Ostien, Variational Nonlocal Regularization, *in prep*

# Regularization

Length scale comes from thickness parameter

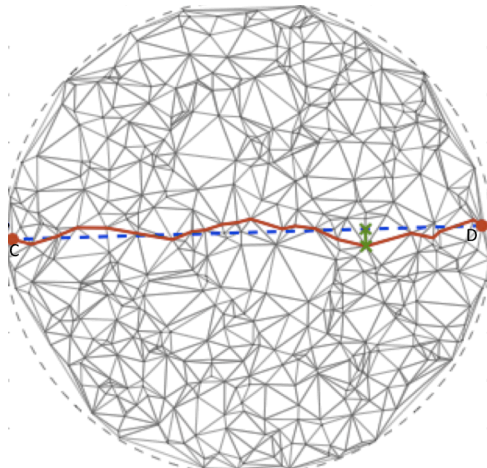
## ■ Surface elements

$$\begin{aligned}
 \mathbf{F}^\perp &= \mathbf{I} + \frac{[\Phi]}{h} \otimes \mathbf{N} \\
 \mathbf{F}^\perp &\rightarrow \text{Diagram showing decomposition of } \mathbf{F}^\perp \text{ into } \hat{\mathbf{G}}_3 = \hat{\mathbf{N}} \text{ and } \mathbf{B}_I \\
 \mathbf{F}^\parallel &= \mathbf{g}_i \otimes \hat{\mathbf{G}}^i \\
 \mathbf{F} &= \mathbf{F}^\parallel \mathbf{F}^\perp \\
 \hat{\mathbf{G}}_A \parallel \mathbf{G}_A &\longrightarrow \mathbf{F} = \mathbf{F}^\parallel + \frac{[\varphi]}{h} \otimes \mathbf{N}
 \end{aligned}$$

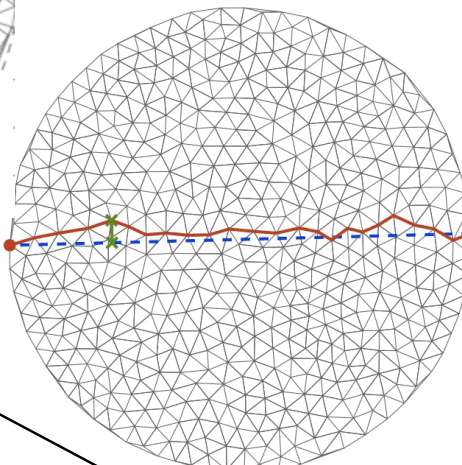


Regularized global solution solution

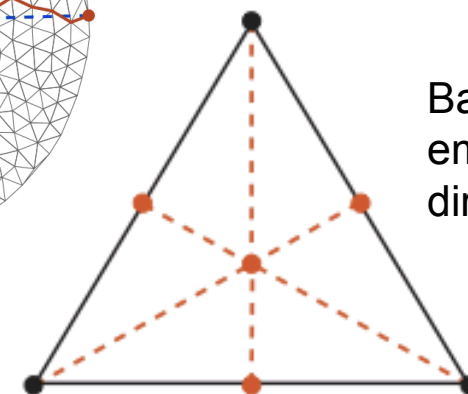
# Review of optimal meshes, Rimoli & Rojas



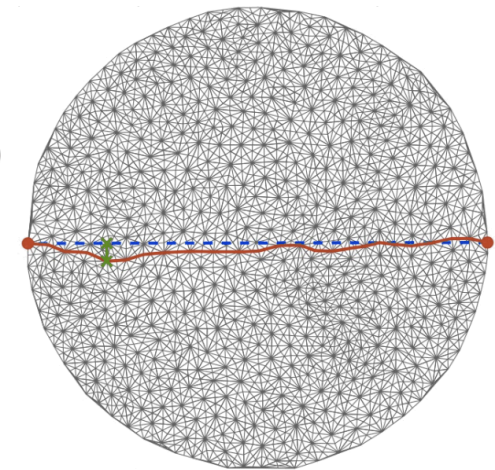
A random mesh is generated by throwing random points and performing Delaunay's triangulation.



A K-means clustering algorithm is used to improve the mesh quality of the random mesh



Barycentric subdivision is employed to add conjugate directions to the mesh



*Goal: Minimize error between  
"true" path and discrete path*

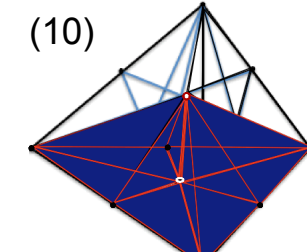
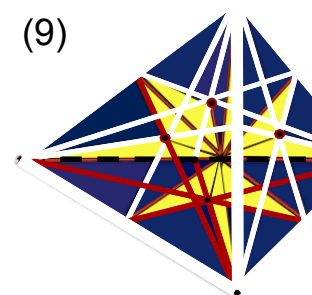
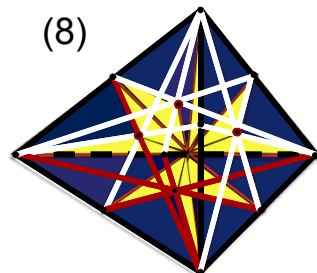
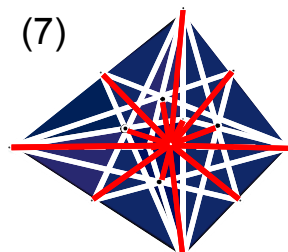
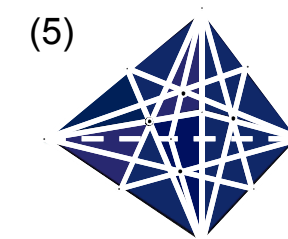
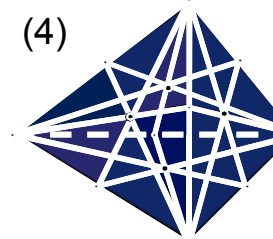
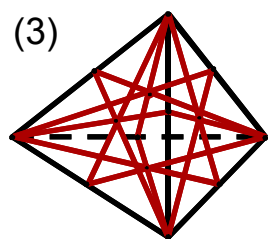
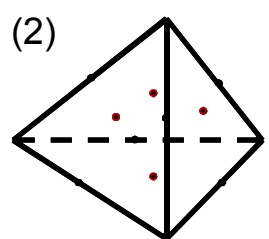
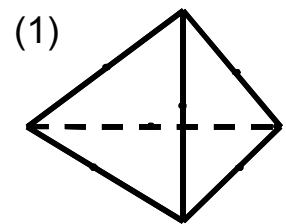
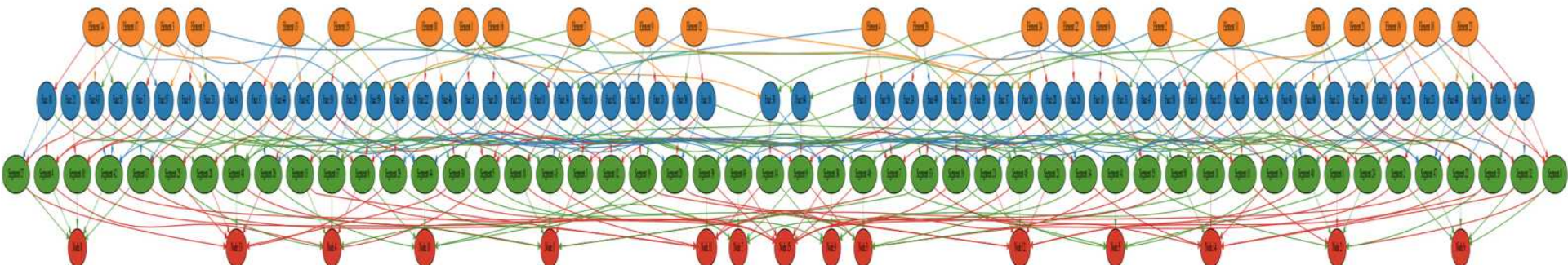
— “true” path

— discrete path

— geometric error (Hausdorff distance)

# Evolution of barycentric subdivision in 3-D (10)

(10) Add the corresponding new elements



# Bifurcation

- Surface insertion criteria evaluated on interior faces

Define the acoustic tensor

$$A := n \cdot \mathbb{C} \cdot n, \quad n \in S^2$$

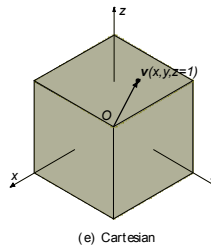
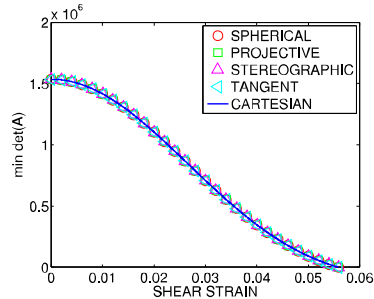
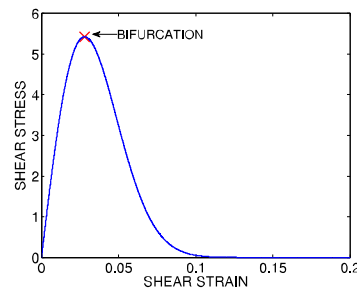
The strong ellipticity condition

$$m \cdot A \cdot m > 0, \quad m \in S^2$$

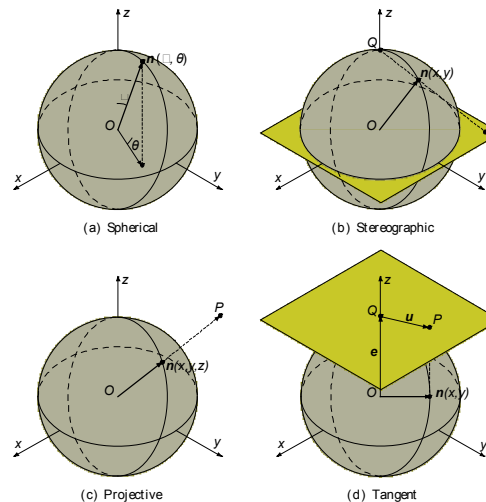
The bifurcation condition to determine the onset of material failure

$$\det A > 0$$

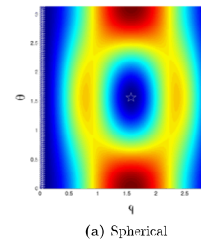
## Simple Shear



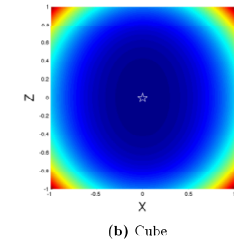
## Parameterizations of the unit sphere



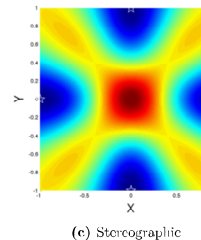
Different landscapes of the determinant emerge as a function of parameterization



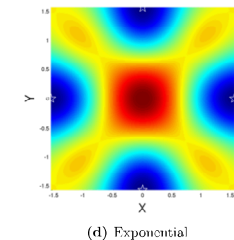
(a) Spherical



(b) Cube



(c) Stereographic



(d) Exponential

Evaluate for accuracy, robustness, efficiency

# Continuum-to-Continuum Coupling



- Methods to couple continuum treatments at different length and time scales
- Two examples
  - Arlequin – Domain coupling via energy partitioning
  - An extension of the variational multiscale method to finite deformation

# Energy Partition – method to describe one mechanical response in one domain with two energy functionals

## Partitioned Incremental Energy Functional

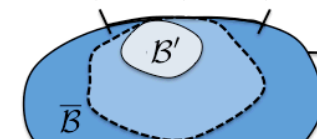
$$\Phi[\bar{\varphi}, \varphi', \phi] = \Phi^{\text{int}}[\bar{\varphi}, \varphi'] - \Phi^{\text{ext}}[\bar{\varphi}, \varphi'] + \Lambda[\bar{\varphi}, \varphi', \phi]$$

$$\Phi^{\text{int}}[\bar{\varphi}, \varphi'] = \int_{\mathcal{B}} \alpha \bar{W}(\bar{\mathbf{F}}, \bar{z}) + (1 - \alpha) W'(\mathbf{F}', z') \, dV$$

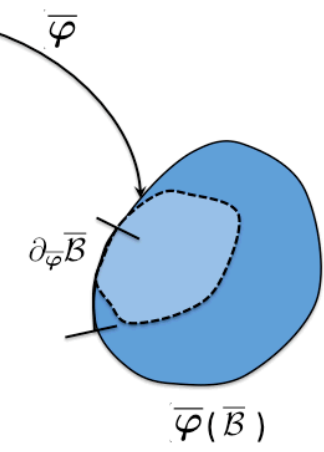
$$\begin{aligned} \Phi^{\text{ext}}[\bar{\varphi}, \varphi'] = & \int_{\mathcal{B}} \beta \rho_0 \bar{\mathbf{B}} \cdot \bar{\varphi} + (1 - \beta) (\rho_0 \mathbf{B})' \cdot \varphi' \, dV \\ & + \int_{\partial_T \mathcal{B}} \beta \bar{\mathbf{T}} \cdot \bar{\varphi} \, dS + \int_{\partial_T \mathcal{B}} (1 - \beta) \mathbf{T}' \cdot \varphi' \, dS \end{aligned}$$

## Partitioned internal energy

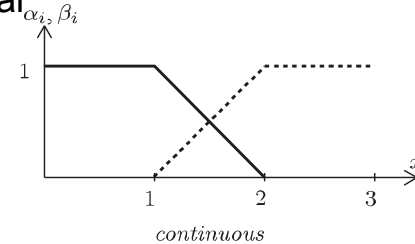
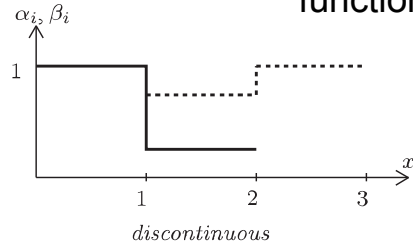
$$\partial_{\varphi} \mathcal{B} = \partial_{\bar{\varphi}} \bar{\mathcal{B}} \cup \partial_{\varphi'} \mathcal{B}'$$



$$\mathcal{B} = \bar{\mathcal{B}} \cup \mathcal{B}'$$



## Weighting function partitioned energy functional



## Partitioned external energy

$$\Lambda[\bar{\varphi}, \varphi', \phi] = \int_{\mathcal{B}^c} \phi \cdot (\bar{\varphi} - \varphi') + \kappa l^2 \text{Grad } \bar{\phi} : (\text{Grad } \bar{\varphi} - \text{Grad } \varphi') \, dV$$

$$\alpha(\mathbf{X}) = \beta(\mathbf{X}) = \begin{cases} 1 & \mathbf{X} \in \bar{\mathcal{B}} \setminus \mathcal{B}^c \\ 0 & \mathbf{X} \in \mathcal{B}' \setminus \mathcal{B}^c \end{cases}$$

Partition of unity

Compatibility constraint energy

Partitioned Domain with overlapping region(s)

Sun, Mota, Domain Coupling for Large Deformation Strain Localization, *in prep*

# Foulk's Singular Bar (2008)

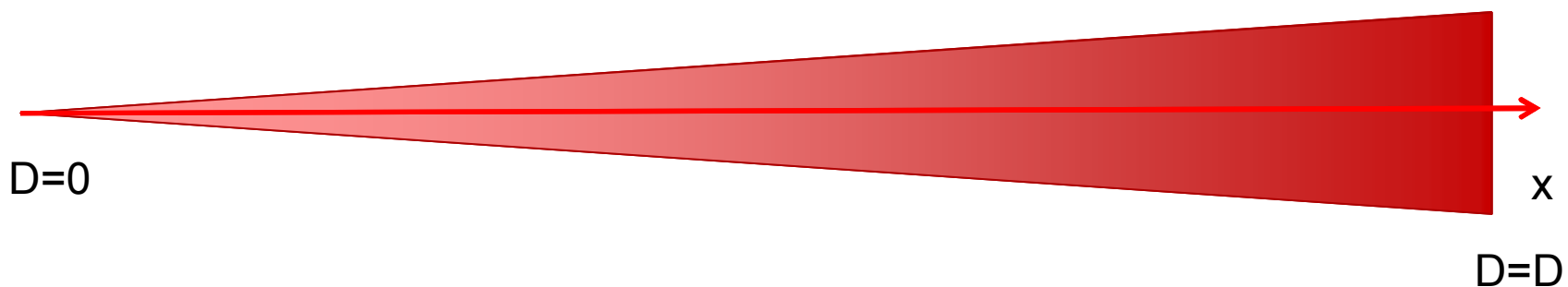
- We use the BVP introduced by James W. Foulk III to test whether regularization procedure is able to regularized the PDE if it is only applied in the fine domain
- Due to the vanishing area, mesh pathology is expected unless length scale is introduced via regularization procedure.

Path dependent damage model

$$W(\mathbf{C}, \zeta) = (1 - \zeta)W_o(\mathbf{C})$$

$$W_o\left(\frac{d\varphi}{dX}\right) = \frac{1}{2}\bar{E}\left(\left(\frac{d\varphi}{dX}\right)^{-2} + \left(\frac{d\varphi}{dX}\right)^2 - 2\right)$$

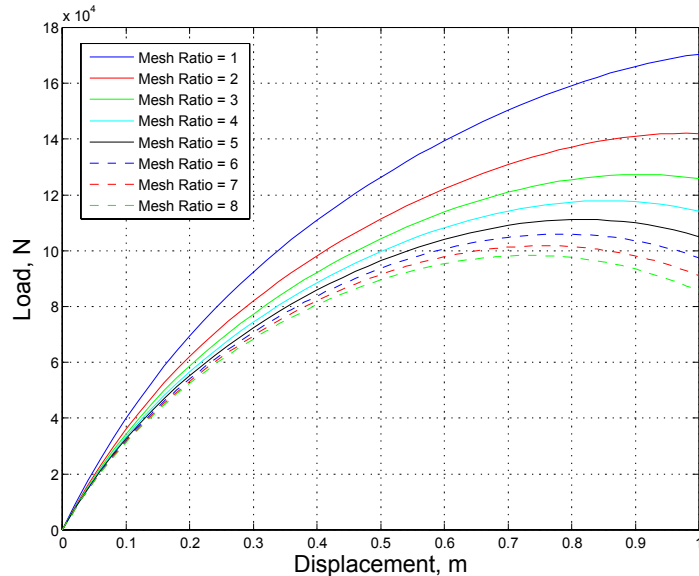
$$\zeta = \zeta(\alpha) = \zeta_\infty[1 - \exp(-\alpha/\varsigma)] \quad \alpha(t) = \max_{s \in [0, t]} W_o(s)$$



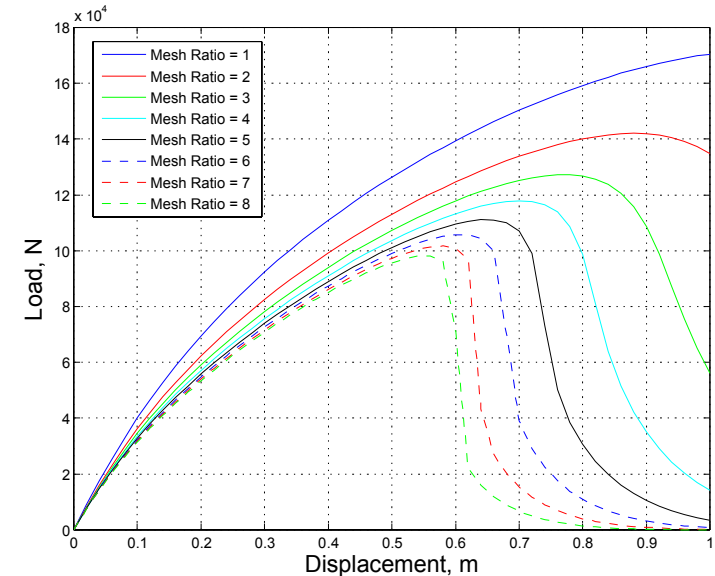
# Example 2 Foulk's bar

## Regularization in small region

With DOC method, only a small nonlocal domain is required to regularize the PDE. A large portion of the domain is modeled by simpler, cheaper constitutive law with coarser mesh to cut down computational cost.



Load-displacement curve with refining nonlocal domain



Load-displacement curve with refining classical domain

# Variational Multiscale

43%- 07'(' ')\*+, - . \*%1 - EE\$%8"

b5 \*34- 0 '7' )\*+, - . \*%, - EE\$%8"

$$X = \bar{\square}(X), \quad x = \square'(X)$$

b\*&07' )\*+, - . \*%, - EE\$%8"

$$\square(X) = \square'(\bar{\square}(X))$$

'%&\*724' "% "34- 0 " ' 0"

$$\delta = x - X$$

$$= \square'(\bar{\square}(X)) - \bar{\square}(X)$$



! 77\$ C '7' 4\*, E\*3\$ \*%"

\*)'7' )\*+, - . \*%, - EE\$%8"

$$\square = \underbrace{\square}_{\text{coarse}} + \underbrace{\delta}_{\text{fine}}$$

1 20 E04- . C '7' 4\*, E\*3\$ \*%"

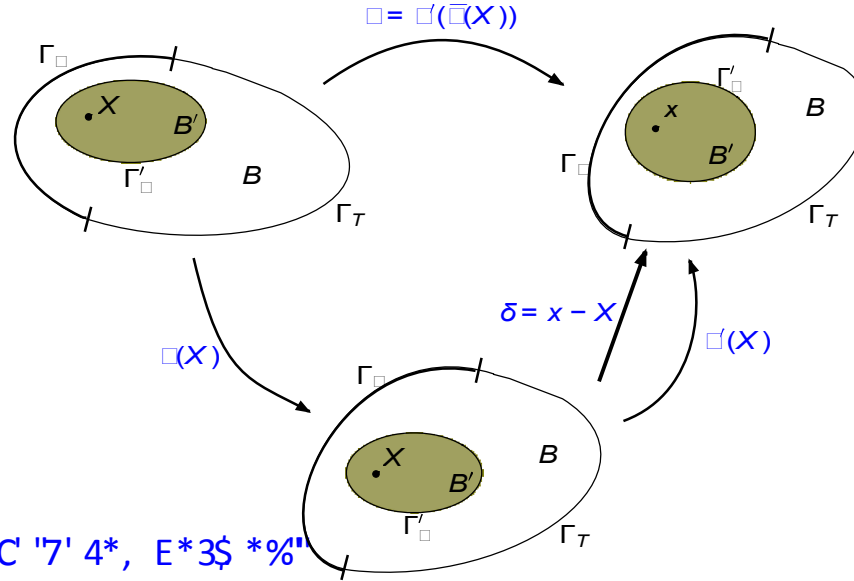
\*)'7' )\*+, - . \*%8+ 7\$ %&

$$F = \frac{\partial x}{\partial X} \frac{\partial X}{\partial X} = F' \bar{F}$$

9, - 03&- \$%4\*%& 2+E- +8X - +\$E- . "- %7'W28=' 3'RMNN?Z - +\$E- . "- %7'W28=' 3'QKKY"

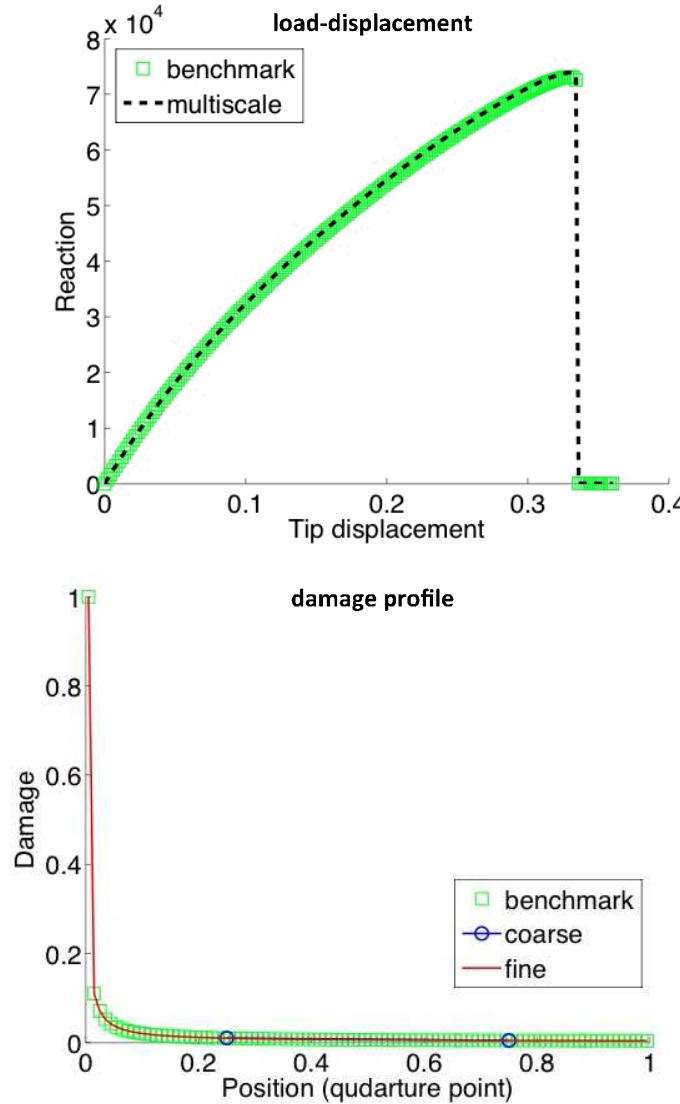
$$u = \bar{u} + u'$$

Decomposition of deformation mapping



# Variational Multiscale

## Hyper-elasticity with damage



- Benchmark solution by full-single scale computation
- Material properties
  - $E = 200 \text{ GPa}$
  - $\nu = 0.25$
  - $\kappa = 133 \text{ GPa}$
  - $\mu = 67 \text{ GPa}$
  - $\xi_\infty = 1.0$
  - $\tau = 100 \text{ GJm}^{-3}$

# Computing Environments

- Sandia's production analysis code suite, Sierra and Sierra/Mechanics
  - Surface (localization) elements
  - Active work on the Nonlocal partitioning algorithm
- Research goes into an open source finite element code repository, Albany
  - Coupled physics (not shown)
  - Adaptivity (not shown)

# Summary and Conclusions

- Multiple efforts towards modeling ductile material behavior up to and including fracture and failure
- Developing and testing non-standard finite elements and methods
- Relying on regularization methods, introducing length scales, resolving plasticity
- The nature of plasticity and ductile failure requires multiple scales to be resolved